

## ARTIFICIAL INTELLIGENCE-ENHANCED MULTI-MATERIAL FORM MEASUREMENT FOR ADDITIVE MATERIALS

P. Stavroulakis\*, O. Davies\*, G. Tzimiropoulos†, and R. K. Leach\*

\*Manufacturing Metrology Team, University of Nottingham, Nottingham, UK

†School of Computer Science, University of Nottingham, UK

### Abstract

The range of materials used in additive manufacturing (AM) is ever growing nowadays. This puts pressure on post-process optical non-contact form measurement systems as different system architectures work most effectively with different types of materials and surface finishes. In this work, a data-driven artificial intelligence (AI) approach is used to recognise the material of a measured object and to fuse the measurements taken from three optical form measurement techniques to improve system performance compared to using each technique individually. More specifically, we present a form measurement system which uses AI and machine vision to enable the efficient combination of fringe projection, photogrammetry and deflectometry. The system has a target maximum permissible error of 50  $\mu\text{m}$  and the prototype demonstrates the ability to measure complex geometries of AM objects, with a maximum size of (10  $\times$  10  $\times$  10) cm, with minimal user input.

**Keywords:** Artificial intelligence; data fusion; photogrammetry; fringe projection; deflectometry; segmentation network;

### Introduction

The aerospace, automotive and medical industries are realising the benefits of using non-contact optical three-dimensional (3D) measurement over traditional stylus-based contact methods to control their processes and perform dimensional quality control on their products [1],[2]. Depending on the technology used, non-contact optical measurement can include most if not all of the following benefits: it is non-destructive, has improved speed, increased area of acquisition per measurement cycle and reduced cost [3]. For non-contact optical camera-based techniques especially, the ability to leverage the benefits of readily available AI-based image recognition algorithms to enhance the measurement even further provides an additional benefit over stylus-based contact techniques [4]. Non-contact optical techniques, however, are not a panacea, and for some measurement scenarios, contact stylus-based techniques still need to be used, as optical techniques suffer from lower accuracy, material sensitivity and much higher requirements for data handling and storage [3].

In optical systems, material sensitivity and measurement range can be minimised by changing optical design and hence many different solutions exist [3]. Consequently, there is a large number of different optical techniques for dimensional measurement which have been developed to work at different length scales and for different applications [5]. The selection of the appropriate technique depends on the specific object size, target measurement accuracy and the material of the object that needs to be measured.

One way to improve functionality of 3D measurement instruments is to combine multiple techniques in one setup; however, this requires that the data be combined in one frame of reference,

which adds to the processing time and complexity of the system. In this work, we perform data fusion by using a common reference camera to employ three different camera-based measurement techniques, hence data fusion is performed without the need to register the frames of reference to each other. The techniques employed here are fringe projection (FP), deflectometry (DM) and photogrammetry (PG). These 3D measurement techniques nominally function at a 100 mm to 1 m operating distance and at a 10  $\mu\text{m}$  to 100  $\mu\text{m}$  accuracy [6]. The techniques selected are ideal for many of the object sizes and material types which need to be measured in automotive, aerospace and additive manufacturing [6].

### **Background**

The three chosen measurement techniques operate via different principles and are largely complementary to each other. The principles of operation of all three are analysed in this section:

#### *Fringe projection*

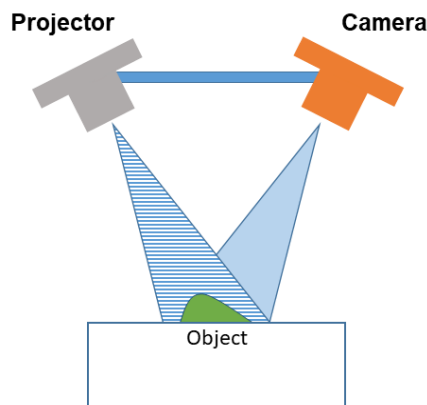


Figure 1. Schema of a fringe projection setup

Fringe projection (Figure 1) is a structured light technique which uses a projector and a camera to create a 3D point cloud of a scene observed by a camera either by triangulation (projecting digital fringes) or phase-stepping (sinusoidal fringes). It is used mainly for measuring diffusely reflecting objects [7].

#### *Deflectometry*

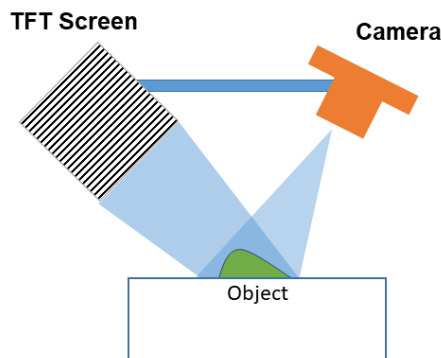


Figure 2. Schema of a deflectometry setup

Deflectometry (Figure 2) is structured light technique similar to fringe projection but instead of projecting the fringe pattern, it is displayed on a TFT screen. This configuration works best for reflective objects, as a bundle of rays from each pixel will reflect from the object into the camera via direct reflection. The types of patterns which are usually used are similar to fringe projection [8]

### *Photogrammetry*

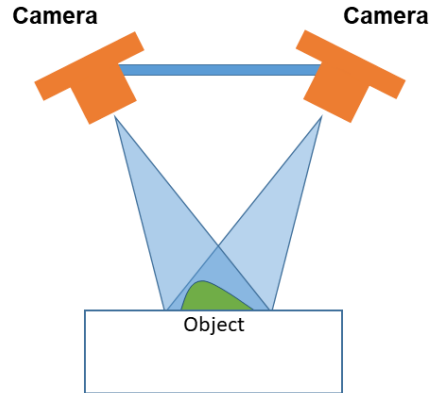


Figure 3. Schema of a photogrammetry setup

Photogrammetry (Figure 3) is a technique which creates a 3D point cloud by taking advantage of unique surface features that exist in two or more images of the object taken from different points of view [9]. Multiple camera views are used in order to reconstruct the 3D surface of an object by searching for pixel correspondences in the images taken.

In this work, the fringe projection and deflectometry systems use phase stepping (project sinusoidal patterns). The photogrammetry system performs triangulation via feature matching [10]. Fringe projection is most effective on featureless objects, whereas photogrammetry is most effective on objects with a large number of features which can easily be detected by computer vision techniques (e.g. SIFT algorithm) in the image. In terms of speed, photogrammetry usually requires a larger number of calculations to perform dense reconstruction and is, therefore, slower in reconstructing the full 3D point cloud than the other two methods. Lastly, deflectometry is most effective for highly reflective objects in comparison to the other two techniques, which require diffusely scattering objects. Hence, by combining these three techniques, 3D surface point clouds can be acquired for reflective and diffuse objects which can be featureless or have multiple features on the surface.

### **Data fusion**

To combine the data from all three 3D measurement techniques, we used the same reference camera for all three systems (Figure 4) and a spatio-temporal data collection scheme to collect data from different parts of the image at different times. This scheme has two parts: an image segmentation strategy and a temporal synchronisation strategy.

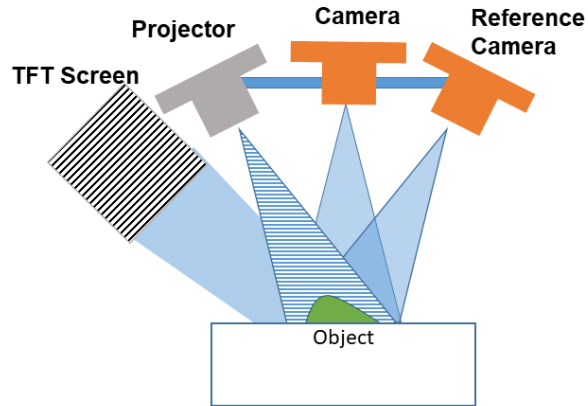


Figure 4. Schema of the combined setup created

### *Image segmentation strategy*

The image segmentation strategy which was selected employs deep learning through a segmentation network (SegNet) and was trained to identify different materials in an image of the scene taken by the reference camera. Matlab was used as the framework for building, training and testing the network. The network used was an uninitialised semantic image segmentation network based on the SegNet architecture [11], consisting of encoding layers that downsample the input image by a factor of four and corresponding decoding layers that upsample back to the input size; the RGB images had  $201 \times 152$  pixels to keep the original aspect ratio whilst being small enough to fit the mini-batch into GPU memory during training. Three material classes were trained by acquiring 400 images of each material, and ground truth images of these were obtained by removing the green background through colour thresholding. The class weighting of the final classification layer used inverse frequency weighting of the total pixel count of each class in the ground truth images.

Of the 1200 images, 81% were used for training, with 9% set aside for validation and 10% for final testing. Random image augmentation was also used to artificially increase the number of training images, consisting of random rotations up to  $360^\circ$ , random reflections horizontally and vertically, and random translations by up to ten pixels horizontally and vertically. The network was trained using an initial learning rate of 0.0005 and a mini-batch size of thirty-two images.

In this manner, all the pixels in an image could be labelled by predicted material class using the trained network and a mask for each was created (Figure 5a-b). As the reference image pixels have essentially been classified according to material, the point clouds could now be created only in specific regions by implementing the correct image mask for each measurement method. Therefore, to optimise the measurement success and associate each measurement technique with a specific material, the Ti6Al-4V mask was used when measuring via photogrammetry (Figure 5c), the carbon fibre mask was used when measuring with deflectometry (Figure 5d) and the polymer mask was used when measuring with fringe projection (Figure 5e).

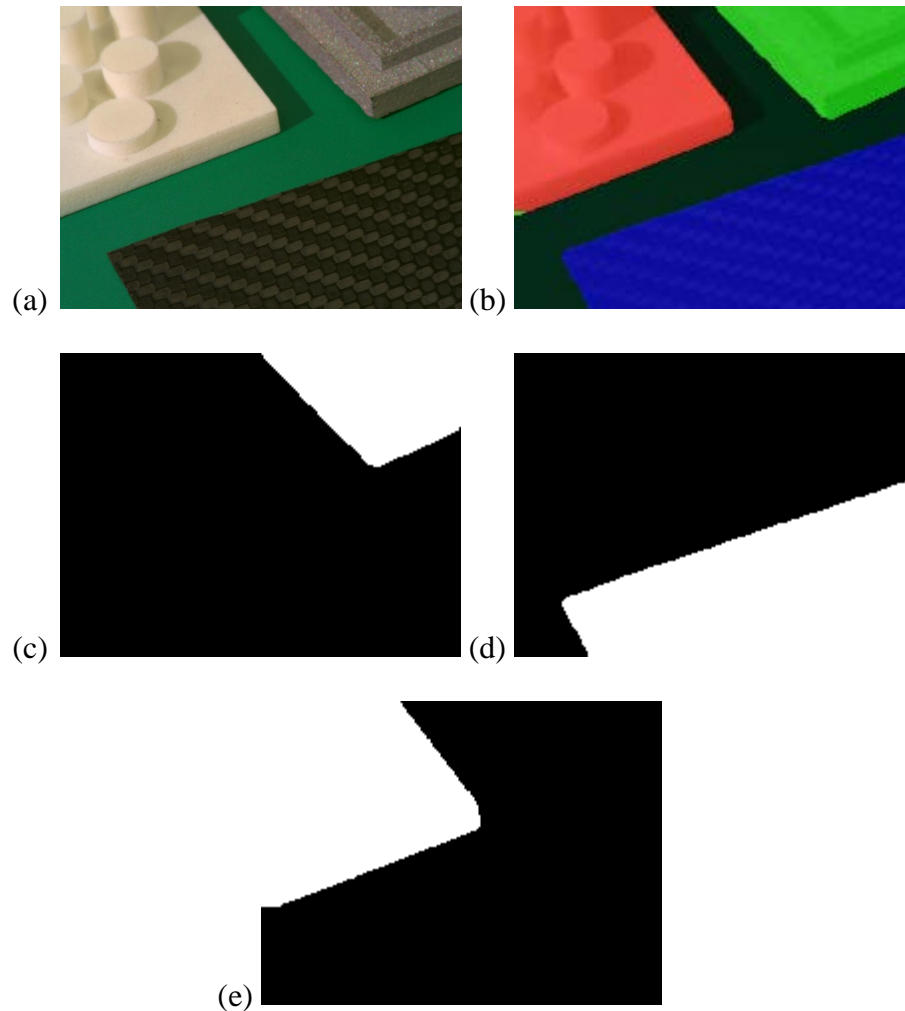


Figure 5. Results of image segmentation of a scene containing polymer, titanium, and carbon fibre objects. Showing (a) initial image, (b) image segmentation overlay results, and three masks created for (c) titanium, (d) carbon fibre, and (e) polymer

### *Temporal synchronisation scheme*

The temporal synchronisation scheme used consists of cycling all three measurement sub-systems (fringe projection, deflectometry and photogrammetry) in the time domain by activating the required modules used by each technique (projector, TFT screen, rotation stage) at the appropriate time and taking measurements of the scene. Before cycling the measurement techniques though, an image of the scene is taken in order to segment the regions of the image which will be used by each technique. Thereby three measurement masks are made and are used by each technique in turn to reconstruct a selected group of pixels which have the best chance of working and ignore the rest.

As all three point clouds are taken by the same reference camera, they are automatically placed in the same frame of reference. The partial 3D data can, therefore, be automatically fused together to form an optimised 3D point cloud of the scene containing all three objects. This

temporal synchronisation strategy allows for both optimised data fusion, minimisation of measurement data and reduction of noise, as each measurement technique works best for a specific material.

## Results

Some of the challenges encountered during the image segmentation strategy were primarily related to spurious reflections and ambient light changes. Below we have identified three cases which needed to be taken into account when training and segmenting the images.

### *Case 1: Reflections from objects in the scene*

In Figure 6, the effect of reflections from objects of a different class is shown. Regions of the carbon fibre object are confused for being parts of the metal material class.

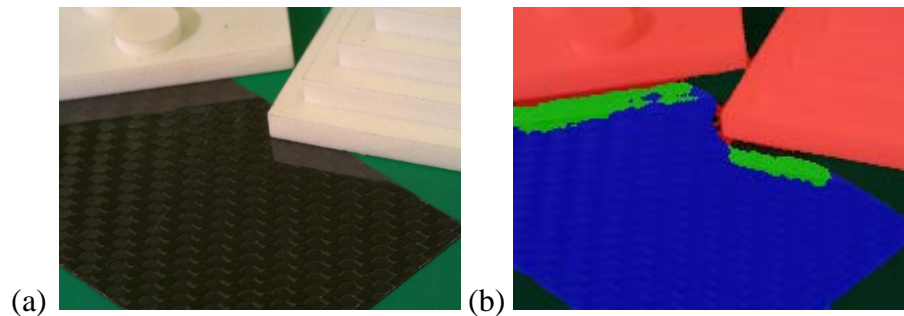


Figure 6. Mistakes in prediction caused by reflections of other objects from the carbon fibre surface with (a) initial image and (b) image segmentation overlay results.

### *Case 2: Reflections from environmental lighting*

In Figure 7, the effect of ambient lamp reflections is shown. Regions of the carbon fibre object are confused for being parts of the polymer and titanium material class.

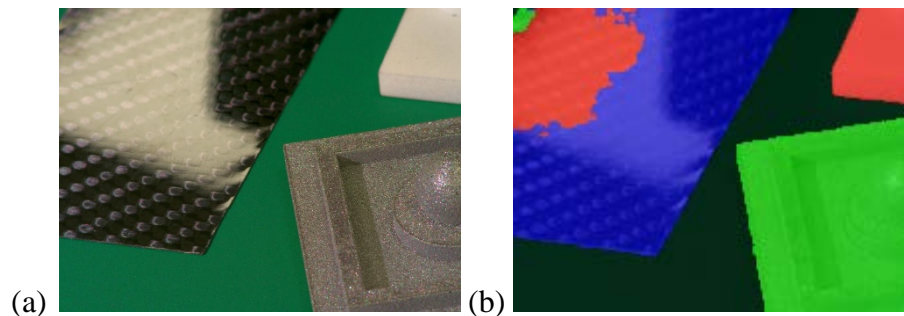


Figure 7. Mistakes in prediction caused by ambient lamp reflections from the carbon fibre surface with (a) initial image and (b) image segmentation overlay results.

### Case 3: Illuminating objects with different lighting scheme

In Figure 8, the effect of applying a different lighting scheme to that used in the original training scheme is shown. Regions of the carbon fibre object are confused for being a part of the background, and the shadow from titanium and polymer objects are confused for being a part of the titanium material class.

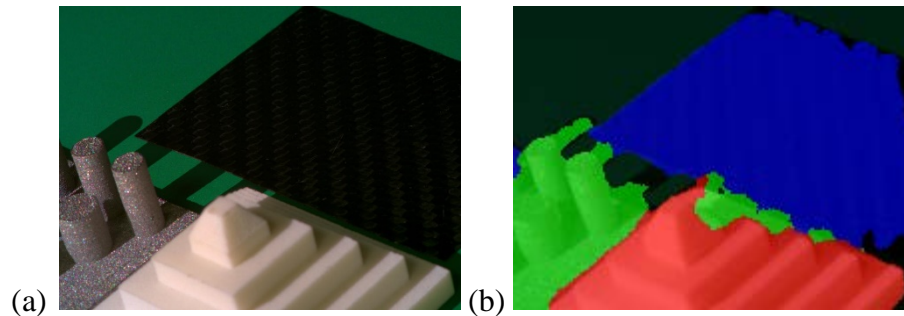


Figure 8. Mistakes in prediction caused by illuminating the objects with a different lighting scheme (projector) to that used during the training phase (ambient room lighting).

### Discussion

In this work, an investigation into detecting different AM object materials via use of AI segmentation has been presented. Specifically, the detection of Ti-V6-Al4, nylon polymer and carbon fibre were investigated. Several problems were identified in the segmentation of the images, which were related to the discrepancies in lighting and reflections which existed when acquiring images from the experimental setup. In particular, reflections from other objects, reflections from ambient light sources and the significant change in lighting create errors in the segmentation of the images by labelling a large proportion of pixels erroneously.

Future work will include controlling the lighting and reflections used when creating the images by shielding the samples from ambient lighting as well as training the network by including more illumination conditions in order to improve robustness and finally customizing the selection of network parameters to enable more accurate segmentation of the images.

### Acknowledgements

This work is sponsored by EPSRC grants EP/M008983/1 and EP/L016567/1 and the EU Framework Programme for Research and Innovation – Horizon 2020 – Grant Agreement No 721383.

### References

- [1] J. E. Muelaner and P. G. Maropoulos, “Large volume metrology technologies for the light controlled factory,” *Procedia CIRP*, vol. 25, pp. 169–176, 2014.
- [2] K. Harding, *Handbook of Optical Dimensional Metrology*. Taylor & Francis, 2013.
- [3] V. Carbone, M. Carocci, E. Savio, G. Sansoni, and L. De Chiffre, “Combination of a vision system and a coordinate measuring machine for the reverse engineering of freeform

- surfaces,” *Int. J. Adv. Manuf. Technol.*, vol. 17, no. 4, pp. 263–271, Jan. 2001.
- [4] R. K. Leach, N. Senin, X. Feng, P. Stavroulakis, R. Su, W. P. Syam, and T. Widjanarko, “Information-rich metrology: changing the game,” *Commer. Micro Manuf.*, vol. 8, pp. 33–39, 2017.
- [5] G. Sansoni, M. Trebeschi, and F. Docchio, “State-of-the-art and applications of 3D imaging sensors in industry, cultural heritage, medicine, and criminal investigation,” *Sensors*, vol. 9, no. 1, pp. 568–601, 2009.
- [6] P. I. Stavroulakis and R. K. Leach, “Invited Review Article: Review of post-process optical form metrology for industrial-grade metal additive manufactured parts,” *Rev. Sci. Instrum.*, vol. 87, no. 4, pp. 0411011–04110115, 2016.
- [7] S. Zhang, *High-Speed 3D Imaging with Digital Fringe Projection Techniques*. CRC Press, 2016.
- [8] M. Servin, A. Quiroga, and M. Padilla, *Fringe Pattern Analysis for Optical Metrology*. Wiley-VCH, 2014.
- [9] R. Hartley and A. Zisserman, *Multiple View Geometry in Computer Vision*, 2nd Ed. Cambridge University Press, 2004.
- [10] D. Sims-Waterhouse, P. Bointon, S. Piano, and R. K. Leach, “Experimental comparison of photogrammetry for additive manufactured parts with and without laser speckle projection,” in *Proc. SPIE 10329, Optical Measurement Systems for Industrial Inspection X*, 2017, p. 103290W.
- [11] V. Badrinarayanan, A. Kendall, and R. Cipolla, “SegNet: A deep convolutional encoder-decoder architecture for image segmentation,” *IEEE Trans. Pattern Anal. Mach. Intell.*, vol. 39, no. 12, pp. 2481–2495, Dec. 2017.